

MedChemComm

Accepted Manuscript



This article can be cited before page numbers have been issued, to do this please use: Y. Zhang, G. L. V. Damu, S. Cui, J. Mi, V. K. R. Tangadanchu and C. Zhou, *Med. Chem. Commun.*, 2017, DOI: 10.1039/C7MD00112F.



This is an Accepted Manuscript, which has been through the Royal Society of Chemistry peer review process and has been accepted for publication.

Accepted Manuscripts are published online shortly after acceptance, before technical editing, formatting and proof reading. Using this free service, authors can make their results available to the community, in citable form, before we publish the edited article. We will replace this Accepted Manuscript with the edited and formatted Advance Article as soon as it is available.

You can find more information about Accepted Manuscripts in the [author guidelines](#).

Please note that technical editing may introduce minor changes to the text and/or graphics, which may alter content. The journal's standard [Terms & Conditions](#) and the ethical guidelines, outlined in our [author and reviewer resource centre](#), still apply. In no event shall the Royal Society of Chemistry be held responsible for any errors or omissions in this Accepted Manuscript or any consequences arising from the use of any information it contains.



ARTICLE

Received 00th January
20xx,

Accepted 00th January 20xx

DOI: 10.1039/x0xx00000x

www.rsc.org/

Discovery of potential antifungal triazoles: Design, synthesis, biological evaluation, and preliminary antifungal mechanism exploration†‡

Yuan Zhang,[§] Guri L V Damu,^{§#} Sheng-Feng Cui,[§] Jia-Li Mi,^b Vijai Kumar Reddy Tangadanchu^{#a} and Cheng-He Zhou^{*a}

A series of triazoles as miconazole analogues were designed, synthesized and characterized by IR, NMR, MS and HRMS spectra. All the newly prepared compounds were screened for their antifungal activities against five fungi. The bioactive assay showed that most of the synthesized compounds exhibited good or even stronger antifungal activities in comparison with reference drugs miconazole and fluconazole. Especially, 3,4-dichlorobenzyl derivative **5b** showed comparable or superior activity against all the tested fungal strains to standard drugs, and formed supramolecular complex with CYP51 *via* the hydrogen bond between the 4-nitrogen of triazole nucleus and histidine residue. Preliminary experiments revealed that both of the active molecules **5b** and **9c** could intercalate into calf thymus DNA, which might block DNA replication to exert their powerful antifungal abilities. The further study indicated that compound **5b** might be stored and transported by human serum albumin through hydrophobic interactions, specific electrostatic interactions and hydrogen bonds. These results strongly suggested that compound **5b** could be served as a promising antifungal candidate.

1. Introduction

The rapidly emerging multidrug resistant microorganisms over the world have exerted a great threat to human health. The development of novel antimicrobial drugs is an important approach to combat the increasingly frequent pathogenic drug resistance,¹ which has been a major task worldwide for medicinal chemists. Currently, the modification of available clinic drugs has been acknowledged to be a prominent method to exploit new drugs with a view of reducing cross resistance.²

Miconazole is the first well-known commercially significant imidazole drug with a structure of α -aryl azolyl ethanol, this drug has a well-established treatment for many mycotic infections with low toxicity and excellent safety profile.³ It has been generally considered that miconazole acts by competitive inhibition *via* directly inhibiting Cytochrome P450 (CYP450)-dependent enzyme, 14 α -lanosterol demethylase (CYP51), which results in a lethal disruption in the normal sterol biosynthesis chain in fungi, but it is of minimal consequence to mammals.⁴ Nevertheless, the shortcomings

of miconazole including the poor aqueous solubility, limited active spectrum, a lack of oral absorption and occasional undesirable side effects when administered at therapeutic doses intravenously, have imposed restriction on its efficacy and administrable mode.⁵ It is conceivable that conformationally constrained miconazole analogues mimicking the bioactive conformation might exhibit a higher level of intrinsic antifungal potency.⁶ Furthermore, the analogues of miconazole or other further structural modification of the analogues, could produce candidates from this series for preclinical progression.⁷ Therefore, much effort has been devoted to its structural modification and the development of its analogues and many excellent achievements have been obtained.⁸ Lots of miconazole analogues such as econazole, fenticonazole, sulconazole and so on have been successfully developed, marketed and extensively used in clinic for the treatment of fungal infection with high safety, low toxicity and few adverse effects.⁹

Triazole nucleus has been playing an important role in anti-infective therapy and especially triazole-based fluconazole as first-choice antifungal drug displays advantages like excellent safety profile, favorable pharmacokinetic characteristics and wide biological activities. A large number of triazole antifungal drugs have been widely used in clinic such as fluconazole, voriconazole, itraconazole and posaconazole.¹⁰ Additionally, the toxicity caused by imidazole antifungal drugs is generally considered to result from its strong coordination potency with Fe²⁺ ion, while triazole with lower electronic density as an isostere of imidazole could helpfully reduce toxicity due to inferior coordination potency to imidazole nucleus.¹¹ The structure activity relationship (SAR) also suggests that the imidazole ring is susceptible to metabolic degradation *in vivo* and the introduction of triazole ring to the third generation azole antifungal

^a Institute of Bioorganic & Medicinal Chemistry, Key Laboratory of Applied Chemistry of Chongqing Municipality, School of Chemistry and Chemical Engineering, Southwest University, Chongqing 400715, PR China. E-mail: zhouch@swu.edu.cn; Fax: +86 23 68254967; Tel: +86 23 68254967

^b People's Hospital of Suining, Sichuan 629000, PR China.

† The authors declare no competing interests.

‡ Electronic supplementary information (ESI) available. See DOI: 10.1039/x0xx00000x

§ These authors contributed equally to this work.

Postdoctoral fellow from Indian Institute of Chemical Technology (IICT), India.

drugs is much less susceptible to metabolic degradation *in vivo* and successfully used in clinic.¹² Furthermore, so far little literature has reported the insertion of triazole ring to miconazole scaffold.

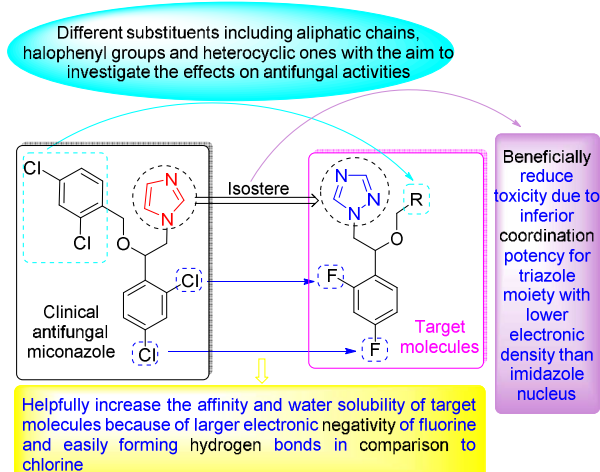
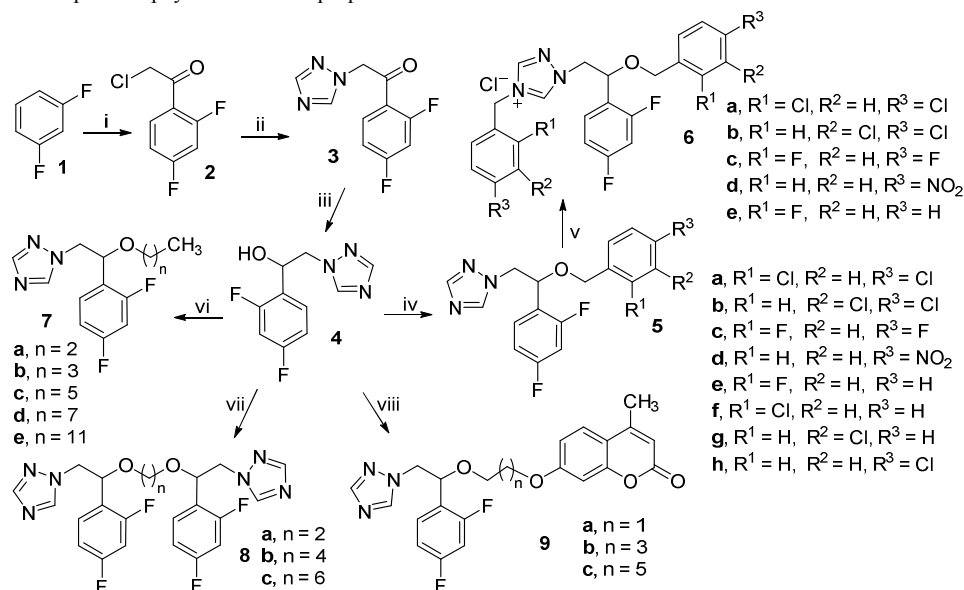


Fig. 1 Design of triazole type of miconazole analogues.

In view of the above observations and on the basis of our previous work on triazoles,¹³ herein we introduced triazole nucleus as isostere of imidazole ring on miconazole, substituted chlorine on benzene ring by fluorine, and replaced dichlorophenyl group of miconazole by alkyl chains with different length, various substituted benzenes and heterocyclic substituents to generate a triazole class of miconazole analogues (Fig. 1). Bis-triazoles have been acknowledged to possess better water solubility, strengthened targeting ability and improved physicochemical properties than

single triazolyl compounds by multi-site binding through the incorporation of another triazole fragment, thus enhancing bioactivities and therapeutic effect.¹⁴ Some bis-triazole antifungal drugs like fluconazole and fosfluconazole have been widely used in clinic with the high stability, low cytotoxicity and efficient administration mode.¹⁵ This encourages the insertion of an additional triazole ring to target framework. Moreover, it is well known that coumarin nucleus has a large conjugated system, possesses desirable electronic and charge-transport properties, and these characteristics result in the extensive potential applications in antimicrobial aspects.¹⁶ In particular, along with the rise of resistant *Candida* strains, the research on coumarins as antifungal alternative have become more and more active.¹⁷ Thereby, coumarin fragment was also incorporated into target molecules to study its contribution to the antifungal activities. Moreover, triazoliums were reported to helpfully improve antimicrobial activity,¹⁸ so some compounds were further transformed into triazoliums. This triazole type of miconazole analogues might be expected to exhibit large potentiality against fungal strains. Therefore, all the newly synthesized compounds were evaluated *in vitro* for their antifungal activities and the SAR was also discussed. The supramolecular interaction of the most active molecule with miconazole-targeting CYP51 was investigated, and deoxyribonucleic acid (DNA) was selected as a target to further explore the possible antifungal mechanism by studying the interaction with the active compounds. The binding behavior of the active compound with human serum albumin (HSA) by experimental and computational methods was performed in order to understand its absorption, distribution, and metabolism.



Scheme 1. Reagents and conditions: (i) ClCH_2COCl , AlCl_3 , CH_2Cl_2 , 20 °C; (ii) triazole, K_2CO_3 , CH_3CN , 25–0 °C; (iii) NaBH_4 , MeOH , 0–25 °C, 4 h; (iv) substituted benzyl halides, NaH , dry THF, N_2 , 0–74 °C, 5–7 h; (v) substituted benzyl halides, K_2CO_3 , CH_3CN , 80 °C, 8–12 h; (vi) alkyl halides, NaH , dry THF, N_2 , 0–45 °C, 4–6 h; (vii) NaH , dry THF, dibromoalkanes, N_2 , 0–45 °C, 6–8 h; (viii) NaH , dry THF, N_2 , coumarin alkyl halides, 0–75 °C, 8–12 h.

2. Chemistry

Commercially available *m*-difluorobenzene **1** was acylated to produce intermediate **2**, and then was reacted with the

weak base potassium carbonate to afford triazole derivative **3** in a high yield of 85%. Compound **3** was reduced with sodium borohydride to yield the triazolyl ethanol **4** in an almost quantitative yield of 97%, which was further treated with a series of substituted

benzyl halides in dry tetrahydrofuran (THF) using sodium hydride as base under the atmosphere of nitrogen to afford the corresponding ether triazoles **5a–h** with yields ranging from 33.4% to 92.9% and alkyl triazole derivatives **7a–e** with yields of 21.9–75.6%. Bis-triazoles **8a–c** in yields of 62.1–67.2% could be obtained by nucleophilic substitution of triazolyl ethanol **4** with dibromoalkanes. Coumarin alkyl halides¹⁹ were coupled with triazolyl alcohol **4** to produce coumarin derivatives **9a–c** with yields of 42.6–62.6%. The further quaternization of triazoles **5a–h** by halobenzyl halides produced the corresponding triazoliums **6a–e** in moderate to good yields after purification. All the new synthesized conjugates were characterized using IR, ¹H NMR, ¹³C NMR, MS and HRMS (ESI[±]).

3. Results and discussion

3.1 Antifungal activities

The obtained results were depicted in Table 1. Minimal inhibitory concentration (MIC, µg/mL) is defined as the lowest concentration of target compounds that completely inhibited the growth of fungi (provided by the School of Pharmaceutical Sciences, Southwest University and the College of Pharmacy, Third Military Medical University), and determined by means of standard two-fold serial dilution method in 96-well microtest plates according to the National Committee for Clinical Laboratory Standards (NCCLS).²⁰ Table 1 revealed that most of the newly synthesized triazoles showed comparable or even superior inhibitory activities against all the tested fungal strains to standard drugs fluconazole and miconazole except for compounds **4**, **5d**, **6c**, **8c** and **9a** without obvious antifungal efficacy.

The substitution of hydroxyl group in compound **4** by halobenzyl halides yielded the triazole type of miconazole analogues **5a–h** (MIC = 0.5–32 µg/mL) with comparable or even superior inhibitory activities against all the tested fungal strains to standard drugs fluconazole (MIC = 1–16 µg/mL) and miconazole (MIC = 4–32 µg/mL) except for 4-nitrobenzyl compound **5d** with MICs more than 256 µg/mL. Especially compounds **5a**, **5b**, **5c** and **5e** could efficiently inhibit the growth of *A. flavus* strain *in vitro* with MIC values ranging from 8 to 16 µg/mL, which were 16-fold and 32-fold more active than fluconazole and miconazole (MIC = 256 µg/mL) respectively. *B. yeast* strain was quite sensitive to target compounds **5a** (MIC = 8 µg/mL), **5b** (MIC = 0.5 µg/mL) and **5c** (MIC = 4 µg/mL) in comparison with miconazole (MIC = 32 µg/mL) and fluconazole (MIC = 16 µg/mL) and it was apparent that 3,4-dichlorobenzyl compound **5b** exhibited the highest antifungal activity among these conjugates, which was 64-fold more potent than miconazole. Prominently, the 3,4-dichlorobenzyl derivative **5b** displayed not only stronger antifungal efficacies, but also broader bioactive spectrum against all the tested strains at low inhibitory concentrations (MIC = 0.5–8 µg/mL) in comparison with references fluconazole and miconazole. This revealed that 3,4-dichlorobenzyl triazole **5b** could be served as a lead compound in the development of more effective broad-spectrum antifungal agents. 2,4-Difluorobenzyl triazole also exhibited superior or

comparable efficacies (MIC = 4–16 µg/mL) than miconazole (MIC = 4–256 µg/mL) and prominently its anti-*A. flavus* activity was 16-fold more potent than fluconazole and miconazole. However, 4-nitrobenzyl compound **5d** had nearly no inhibitory potentiality against the tested fungi with MICs more than 256 µg/mL. Additionally, 2-fluorobenzyl miconazole analogue **5e** (MIC = 0.5 µg/mL) gave strong antifungal efficacies against *C. albicans* strain, which was superior to standard drug fluconazole (MIC = 1 µg/mL) and miconazole (MIC = 4 µg/mL). Thus, 2-fluorobenzyl analogue **5e** might be hopeful to be served as a new potential anti-*C. albicans* drug that deserves further investigation. Against fungi *C. utilis* and *B. yeast*, 2-chlorobenzyl compound **5f** and 3-chlorobenzyl compound **5g** showed comparable inhibitory activities with fluconazole (MIC = 8 and 16 µg/mL, respectively), while the 4-chlorobenzyl analogue **5h** presented enhanced potencies in the inhibition of *C. utilis* and *A. flavus* with MIC of 4 and 8 µg/mL respectively as compared to compounds **5f** and **5g**, indicating that the 4-chloro substitution on benzene ring was more beneficial than replacement at other position. It could also be deduced that chloro and fluoro substituents on benzene ring exerted more important influence on antifungal activities than nitro group, since 3,4-dichlorobenzyl compound **5b**, 2,4-difluorobenzyl derivative **5c** and 2-fluorobenzyl miconazole analogue **5e** could effectively inhibit the growth of most tested fungal strains at low concentrations, which were much more effective than nitrobenzyl compound **5d**. It was also noticed that disubstituted benzyl triazoles (MIC = 0.5–16 µg/mL) generally exhibited higher potency than these monosubstituted benzyl compounds (MIC = 0.5–32 µg/mL).

The quaternization of halobenzyl compounds **5a–e** could afford corresponding triazoliums **6a–e**, which got totally decreased antifungal activities in comparison with their precursors **5a–e**. Especially, the ionized product **6c** with MICs more than 256 µg/mL showed much lower efficiencies than 2,4-difluorobenzyl compound **5c** and reference drugs. Therefore, it was suggested that the *N*-3 unsubstituted triazole ring was a necessary functional group to exert the antifungal activity against fungal strains. Nonetheless, most of them with MICs in the range of 16–64 µg/mL showed better anti-*A. flavus* activity than fluconazole and miconazole (MIC = 256 µg/mL). On the other hand, alkyl derivatives **7a–e** exhibited moderate to weak antifungal efficiencies towards the tested fungi in comparison with aryl compound **5a–h** and reference drugs. However, target compounds **7a–e** showed better antifungal activities against *A. flavus* than fluconazole and miconazole. Furthermore, the propyl miconazole analogue **7a** displayed comparable anti-*C. albicans* potencies and 8-fold more potent inhibitory activity against *C. mycoderma* (MIC = 4 and 1 µg/mL, respectively) in comparison with miconazole (MIC = 4 and 8 µg/mL, respectively). Butyl substituted compound **7b** gave comparable or 2-fold more potent potency against *C. utilis* in comparison with fluconazole (MIC = 8 µg/mL) and miconazole (MIC = 16 µg/mL). When the alkyl group was extended to octyl group, the produced octyl derivative **7d** could restrain the growth of *C. albicans* at 4 µg/mL, which was identical to miconazole. The replacement of alkyl substituent with dodecyl group produced dodecyloxy derivative **7e**, which had a 2-fold increased potentiality (MIC = 8 µg/mL) against *B. yeast* in

comparison with standard drug miconazole (MIC = 16 $\mu\text{g}/\text{mL}$). These results indicated that the length of alkyl chain exerted no obvious effects on biological activities. Nevertheless, these alkyl substituted analogues behaved less active than aryl containing compounds, which manifested that aryl groups were more favorable than alkyl chains to some extent.

The incorporation of another triazole fragment at the alkyl end of compounds **7a-c** afforded bis-triazole compound **8a-c** with lower antifungal potencies than **7a-c**. Especially, butyl- and hexyl-bridged bis-triazoles **8b** and **8c** showed middle to poor antifungal activity against all the tested strains. However, compounds **8a-c** generally gave better activities against almost the tested fungi than triazole alcohol **4** and it was noteworthy that propyl-linked bis-triazole **8a** with MIC of 8 $\mu\text{g}/\text{mL}$ displayed comparable or better fungistatic abilities against *C.*

utilis and *B. yeast* to corresponding reference drugs fluconazole and miconazole, which might be a consequence of the shortening of the alkyl linker length between triazole ether. In addition, the substitution of one triazole fragment on compounds **8a-c** by coumarin scaffold could generate coumarins **9a-c** with increased inhibitory efficacies in comparison with **8a-c** and precursor **4**, and especially coumarins **9b** and **9c** containing $(\text{CH}_2)_4$ and $(\text{CH}_2)_6$ moieties exhibited extremely high antifungal activities against *C. albicans* and *C. mycoderma* with MIC values ranging from 1 to 4 $\mu\text{g}/\text{mL}$. Particularly, compound **9c** gave the most prominent anti-*C. mycoderma* activity with MIC of 1 $\mu\text{g}/\text{mL}$ in comparison with standard drugs. It was indicated that in the coumarin series the suitable increase of carbon linker length was favourable to the fungi inhibitory efficacies.

Table 1 *In vitro* antifungal data as MIC ($\mu\text{g}/\text{mL}$) for triazoles **4-9**^a

Comps	Fungi					Comps	Fungi				
	<i>C. utilis</i>	<i>A. flavus</i>	<i>B. yeast</i>	<i>C. albicans</i>	<i>C. mycoderma</i>		<i>C. utilis</i>	<i>A. flavus</i>	<i>B. yeast</i>	<i>C. albicans</i>	<i>C. mycoderma</i>
4	256	>256	>256	128	256	6e	32	64	32	32	8
5a	4	16	8	8	16	7a	32	128	64	4	1
5b	1	8	0.5	1	4	7b	8	128	128	64	64
5c	4	16	4	4	8	7c	16	32	32	64	32
5d	>256	>256	>256	>256	>256	7d	16	128	16	4	16
5e	4	32	16	0.5	2	7e	>256	128	8	>256	>256
5f	8	16	16	8	8	8a	8	256	8	64	256
5g	8	32	16	16	16	8b	128	64	64	128	128
5h	4	8	16	8	16	8c	>256	256	128	256	256
6a	8	32	64	16	32	9a	256	256	128	128	256
6b	32	64	16	32	64	9b	16	32	4	4	2
6c	>256	>256	128	>256	>256	9c	16	16	16	2	1
6d	32	16	64	8	16	Fluconazole	8	256	16	1	4
						Miconazole	16	256	32	4	8

^a *C. utilis*, *Candida utilis*; *A. flavus*, *Aspergillus flavus*; *B. yeast*, *Beer yeast*; *C. albicans*, *Candida albicans*; *C. mycoderma*, *Candida mycoderma*.

3.2 Molecular modeling

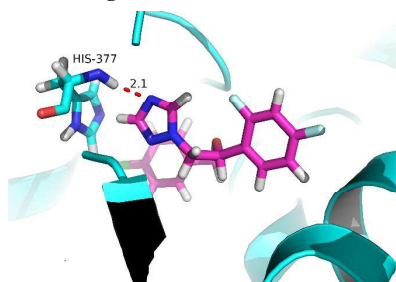


Fig. 2 Three-dimensional conformation of compound **5b** docked in the active site of CYP51.

To further rationalize the observed antifungal activity, a flexible ligand-receptor docking investigation was undertaken. The crystal structure data (CYP51, PDB code: 5V5Z) was obtained from the RCSB protein data bank. Miconazole analogue **5b** was selected to dock with CYP51. According to the docking results (Fig. 2), the binding energy and constant of CYP51 with target compound **5b** is -7.97 kcal/mol and $7 \times 10^5 \text{ M}^{-1}$, respectively. The triazolyl moiety could bind with the active sites of CYP51 through a non-covalent binding mode. Noticeably, the nitrogen atom at 4-position in triazole ring formed hydrogen bond with histidine residue of CYP51.

3.3 Interactions of compounds **5b** and **9c** with calf thymus DNA

DNA as a significant information molecule encoding genetic instructions has been regarded as an important target for studies of bioactive molecules like antimicrobial drugs to explore the possible antimicrobial action mechanism. The interaction studies of compound **5b** (exhibiting good inhibition against all fungal strains) and **9c** with a coumarin scaffold (displaying high efficiency in inhibiting the growth of *C. albicans* and *C. mycoderma*) with calf thymus DNA (Sigma-Aldrich, St. Louis, MO, USA) on molecular level were carried out *in vitro* by UV-vis method.

3.3.1 Absorption spectra of DNA in the presence of compounds **5b** and **9c**

It is well-known that hypochromism and hyperchromism are very important spectral features to distinguish the change of DNA double-helical structure in absorption spectroscopy. The UV-vis spectra (Figs. 3 and 4) showed that the maximum absorption peak of DNA at 260 nm exhibited proportional increase with the increasing concentration of compounds **5b** and **9c**. Furthermore, it was indicated that the measured value of **5b**-DNA complex was a little smaller than the absorption value of the simply sum of free DNA and free compound **5b** (inset of Fig. 3). This meant a weak hypochromic effect existed between DNA and compound **5b**, which was a

consequence of interaction between the electronic states of intercalating chromophore and that of the DNA base, and it also indicated a close proximity of the aromatic chromophore to the DNA bases, while the measured value of **9c**-DNA complex was higher than the sum of free DNA and free compound **9c** (inset of Fig. 4), which suggested a hyperchromism between **9c** and DNA and further proved the conformational change in the DNA duplex. This might be resulted from non-covalent interactions between the complexes and DNA, which led to the part uncoiling of the DNA helix and the exposure of some previously embedded DNA bases.

On the basis of the variations in the absorption spectra of DNA upon binding to **5b** and **9c**, equation 1 can be utilized to calculate the binding constant (K).

$$\frac{A^0}{A - A^0} = \frac{\xi_c}{\xi_{D-C} - \xi_c} + \frac{\xi_c}{\xi_{D-C} - \xi_c} \times \frac{1}{K[Q]} \quad (1)$$

A^0 and A represent the absorbance of DNA in the absence and presence of compounds **5b** and **9c** at 260 nm, ξ_c and ξ_{D-C} are the absorption coefficients of compounds **5b** or **9c** and **5b**-DNA or **9b**-DNA complexes respectively. The plot of $A^0/(A - A^0)$ versus $1/[\text{compound } \mathbf{5b} \text{ or } \mathbf{9c}]$ is constructed by using the absorption titration data and linear fitting (ESI†, Figs. S10 and S11), yielding the binding constant, $K = 1.04 \times 10^4$ or 5.06×10^4 L/mol, $R = 0.9936$ or 0.9964 , $SD = 0.3181$ or 0.0729 respectively (R is the correlation coefficient. SD is standard deviation). Coumarin **9c** had a higher binding constant than triazole **5b**, demonstrating that compound **9c** could combine more tightly with DNA, which might be resulted from the existence of large conjugated coumarin backbone.

3.3.2 Absorption spectra of NR interaction with DNA

Neutral red (NR) as a planar phenazine dye with low toxicity, high stability and convenient application is structurally similar to other planar dyes acridine, thiazine and xanthene and it has been evidenced that the binding of NR with DNA belongs to intercalative binding type.²¹ Therefore, NR was used as a spectral probe to investigate the binding mode of **5b** or **9c** with DNA in this work. The absorption spectrum of NR upon the addition of DNA (ESI†, Fig. S12) indicated that a gradual decrease with the increasing concentration of DNA at absorption peak of NR around 460 nm appeared and a new band around 530 nm developed, which suggested the formation of the new DNA-NR complex. This was further proved by the isosbestic point at 504 nm.

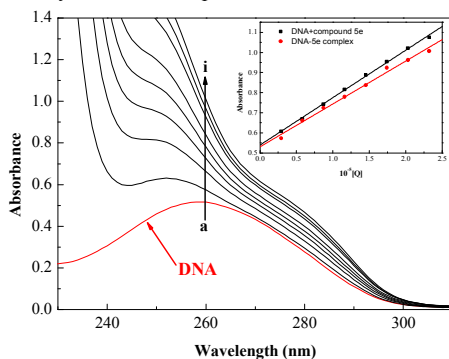


Fig. 3 UV absorption spectra of DNA with different concentrations of compound **5b** at pH 7.4 and room temperature. $c(\text{DNA}) = 5 \times 10^{-5}$ mol/L, and $c(\text{compound } \mathbf{5b}) = 0-2.3 \times 10^{-5}$ mol/L for curves a-i respectively at an increment of 0.29×10^{-5} mol/L. Inset: comparison of absorption at 260 nm

between the **5b**-DNA complex and the sum values of free DNA and free compound **5b**.

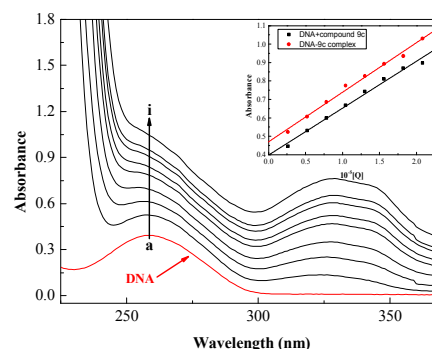


Fig. 4 UV absorption spectra of DNA with different concentrations of compound **9c** at pH 7.4 and room temperature. $c(\text{DNA}) = 5 \times 10^{-5}$ mol/L, and $c(\text{compound } \mathbf{9c}) = 0-2.1 \times 10^{-5}$ mol/L for curves a-i respectively at an increment of 0.26×10^{-5} mol/L. Inset: comparison of absorption at 260 nm between the **9c**-DNA complex and the sum values of free DNA and free compound **9c**.

3.3.3 Absorption spectra of competitive interaction of compounds 5b or 9c and NR with DNA

The competitive binding between NR and **5b** or **9c** with DNA was observed in the absorption spectra (ESI†, Figs. S13 and S14). With the increasing concentration of compound **5b** or **9c**, an obvious intensity increase was observed around 275 nm. In comparison with the absorption around 460 or 530 nm of NR-DNA complex, the absorbance at the same wavelength presented a reverse process (ESI†, inset of Figs. S13 and S14). These various spectral changes suggested that compound **5b** or **9c** could intercalate into DNA by substituting NR in the DNA-NR complex, which might further block DNA replication and thus exert their powerful antifungal activities.

3.4 Iodide quenching experiments

Steady-state quenching could provide further information about the binding mode of a molecule with DNA. It is generally accepted that if a molecule is protected from being quenched in the presence of an anionic quencher due to the repulsion between anionic quencher and the negatively charged phosphate backbone of DNA, the binding mode belongs to intercalation.²² Accordingly, the intercalative binding of the fluorophore should reduce the extent of fluorescence quenching in the DNA environment in comparison to reference solution and hence the value of quenching constant (K_{SV}) of the intercalative bound molecule should be lower than that of the non-intercalative molecule. In this work, KI quenching was introduced to investigate the possible binding mechanism. Quenching curves of compound **5b** in the absence and presence of DNA were shown in Fig. 5 and Fig. 6.

Stern-Volmer equation (2) was used to deduce quenching constant:

$$\frac{F_0}{F} = 1 + K_{SV}[Q] \quad (2)$$

where F_0 and F represent the fluorescence intensity of compound **5b**/**5b**-DNA system in the absence and presence of the quencher KI, respectively. K_{SV} (L/mol) is the Stern-Volmer quenching constant, and $[Q]$ is the concentration of KI. Hence, K_{SV} was calculated by

ARTICLE

Journal Name

linear regression of plot of F_0/F versus $[Q]$. The K_{SV} value of compound **5b** (10.7 L/mol, $R = 0.999$, $SD = 0.019$) in the presence of DNA was lower than that (11.6 L/mol, $R = 0.992$, $SD = 0.067$) in the absence of DNA. It was apparent that iodide quenching effect of compound **5b** by anionic quencher in presence of DNA was decreased, which further evidenced that compound **5b** intercalated into the base pairs of DNA.

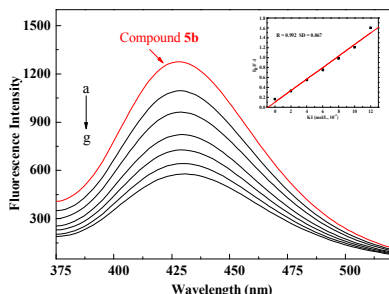


Fig. 5 The fluorescence spectra of compound **5b** with increasing concentration of KI. $c(\text{compound } \mathbf{5b}) = 1.0 \times 10^{-5} \text{ mol/L}$; $c(\text{KI}) = 0-12 \times 10^{-3} \text{ mol/L}$ for curves a-g respectively at an increment of $2 \times 10^{-3} \text{ mol/L}$; red line shows the fluorescence spectrum of compound **5b** only; $T = 298 \text{ K}$, $\lambda_{\text{ex}} = 290 \text{ nm}$. Inset: The Stern-Volmer plot of the fluorescence titration data of compound **5b**.

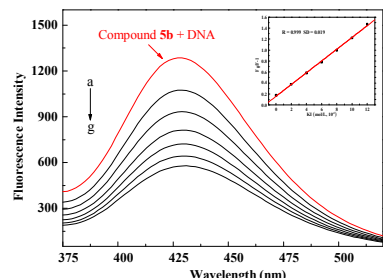


Fig. 6 The fluorescence spectra of compound **5b** and DNA system with increasing concentration of KI. $c(\text{compound } \mathbf{5b}) = 1.0 \times 10^{-5} \text{ mol/L}$; $c(\text{DNA}) = 2.0 \times 10^{-5} \text{ mol/L}$; $c(\text{KI}) = 0-12 \times 10^{-3} \text{ mol/L}$ for curves a-g respectively at an increment of $2 \times 10^{-3} \text{ mol/L}$; red line shows the fluorescence spectrum of compound **5b** and DNA system only; $T = 298 \text{ K}$, $\lambda_{\text{ex}} = 290 \text{ nm}$. Inset: The Stern-Volmer plot of the fluorescence titration data of compound **5b** and DNA system.

3.5 Binding behavior of compound **5e** with HSA

The investigations of interactions between drugs or bioactive small molecules and HSA are not only beneficial to provide a proper understanding of the absorption, transportation, distribution, metabolism and excretion properties of drugs, but also significant to design, modify and screen drug molecules.²³ Therefore, the binding behavior between compound **5e** and HSA (Sigma-Aldrich, St. Louis, MO, USA) was investigated (Fig. 7). It was obvious that HSA had a strong fluorescence emission with a peak at 348 nm owing to the single Trp-214 residue. The intensity of this characteristic broad emission band regularly decreased with the increasing concentrations of compound **5b**, but the maximum emission wavelength of HSA remained unchanged. This suggested that Trp-214 did not undergo any change in polarity, and hence compound **5b** was likely to interact with HSA *via* the hydrophobic region located in HSA.

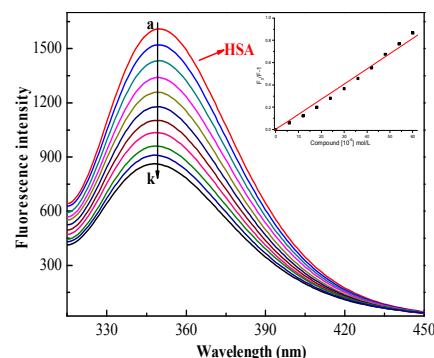


Fig. 7 Emission spectra of HSA in the presence of various concentrations of compound **5b**: $c(\text{HSA}) = 1.0 \times 10^{-5} \text{ mol/L}$; $c(\text{compound } \mathbf{5b}) = 0-2.0 \times 10^{-5} \text{ mol/L}$ for curves a-k at an increment of $0.20 \times 10^{-5} \text{ mol/L}$; blue dash line shows the emission spectrum of compound **5b** only; $T = 286 \text{ K}$, $\lambda_{\text{ex}} = 295 \text{ nm}$.

The fluorescence quenching data can also be analyzed by the well-known Stern-Volmer equation (2):

$$\frac{F_0}{F} = 1 + K_{SV}[Q] = 1 + K_q\tau_0[Q] \quad (2)$$

where F_0 and F represent fluorescence intensity in the absence and presence of compound **5b**, respectively. K_q is the bimolecular quenching rate constant (L/mol/s), τ_0 is the fluorescence lifetime of the fluorophore in the absence of quencher, assumed to be $6.4 \times 10^{-9} \text{ s}$ for HSA, and $[Q]$ is the concentration of compound **5b**. The results also manifested that the binding constants were moderate. Therefore, compound **5b** might be stored and carried by HSA.

Molecular docking evaluation was also performed to understand the binding mode between compound **5b** and HSA. The docking mode was shown in Fig. 8 with the lowest binding free energy and binding constant of -17.32 kJ/mol and $6 \times 10^4 \text{ M}^{-1}$, respectively. As clearly evidenced, compound **5b** was surrounded by Lys-413, Lys-541, Arg-410, Eu-418, Ala-406, Trp-214 and Thr-540. Moreover, compound **5b** partly occupied subdomain IIA, resulting in fluorescence quenching of Trp-214. Hydrophobic interactions existed between the aromatic ring of compound **5b** and HSA. Except for the hydrophobic contacts, hydrogen bonds of 2-F, 4-F on benzene ring as well as 4-N atom on triazole ring with Lys-413, Lys-541 and Ala-406 in HSA and specific electrostatic interactions and were also involved in the binding process. All these indicated that the simulation results coincided well with the above experimental analysis.

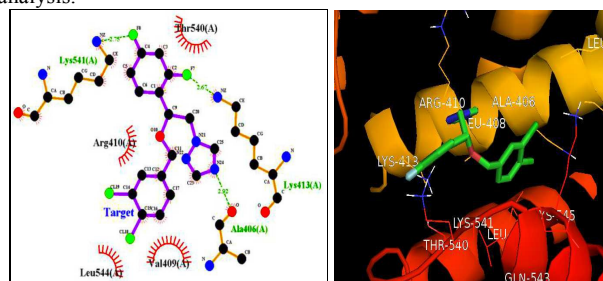


Fig. 8 Hydrophobic pocket of HSA-target and binding model of compound **5b** to HSA.

4. Conclusion

A triazole class of miconazole analogues were designed and synthesized in good yields *via* an easy, convenient and efficient synthetic route. All the newly synthesized compounds were characterized by IR, ¹H NMR, ¹³C NMR, MS and HRMS spectra. The *in vitro* antifungal activities of these miconazole analogues were evaluated against five fungal strains. The biological results revealed that most of the new target compounds exhibited moderate to good antifungal activities against most of the tested strains in comparison with the reference drug miconazole. Especially the 3,4-dichlorobenzyl triazole compound **5b** displayed not only stronger antifungal efficacies, but also broader bioactive spectrum against all the tested strains at low inhibitory concentrations (MIC = 0.5–8 µg/mL) in comparison with miconazole. SAR suggested that both the *N*-3 unsubstituted triazole ring and the substituents on ether linkage were important influence factors on antifungal potency and the introduction of chlorine to benzene ring would improve the fungi inhibitory effect. The docking study showed that the highly bioactive miconazole analogue **5b** could bind with the active sites of CYP51 through the formation of hydrogen bond with histidine residue. The interactive investigations with DNA validated that both of the two active molecules **5b** and **9c** could effectively intercalate into calf thymus DNA to form compound–DNA complexes, which might block DNA replication to exert their powerful antifungal abilities. The binding behaviors and molecular modeling of compound **5b** with HSA suggested that compound **5b** might be stored and transported by HSA, where the hydrophobic interactions, specific electrostatic interactions and hydrogen bonds played important roles. All of these indicated that compound **5b** was a promising antifungal candidate with good curative effect. Further researches, including the *in vivo* bioactive evaluation, time-kill kinetic assay, toxicity, drug resistance and some effect factors on antifungal activities such as other heterocyclic azole rings (benzotriazole, thiazole, oxazole and their derivatives) linked at methylene end are now in progress in our group.

Acknowledgements

This work was partially supported by National Natural Science Foundation of China [(No. 21372186, 21672173)], the Research Fund for International Young Scientists from International (Regional) Cooperation and Exchange Program (No. 81250110089, 81350110338)] and Chongqing Special Foundation for Postdoctoral Research Proposal (Xm2016039). The authors thank Prof. S. Rajagopal from Department of Plant Sciences, School of Life Sciences, University of Hyderabad, India for the help in docking study.

Conflict of Interest

The authors declare no competing author

Notes and references

- (a) I. Levin-Reisman, I. Ronin, O. Gefen, I. Braniss, N. Shores and N. Q. Balaban, *Science*, 2017, **355**, 826–830; (b) E. D. Brown and G. D. Wright, *Nature*, 2016, **529**, 336–343; (c) L. Zhang, X. M. Peng, G. L. V. Damu, R. X. Geng and C. H. Zhou, *Med. Res.*

- Rev.*, 2014, **34**, 340–437.
- (a) D. González-Calderón, M. G. Mejía-Dionicio, M. A. Morales-Reza, A. Ramírez-Villalva, M. Morales-Rodríguez, B. Jauregui-Rodríguez, E. Díaz-Torres, C. González-Romero and A. Fuentes-Benites, *Eur. J. Med. Chem.*, 2016, **112**, 60–65; (b) H. Z. Zhang, L. L. Gan, H. Wang and C. H. Zhou, *Mini-Rev. Med. Chem.*, 2017, **17**, 122–166; (c) W. W. Gao, S. Rasheed, V. K. R. Tangadanchu, Y. Sun, X. M. Peng, Y. Cheng, F. X. Zhang, J. M. Lin and C. H. Zhou, *Sci. China Chem.*, 2017, **60**, 769–785.
- (a) K. De Cremer, K. De Brucker, I. Staes, A. Peeters, F. Van den Driessche, T. Coenye, B. P. A. Cammue and K. Thevissen, *Sci. Rep.*, 2016, **6**, e27463; (c) X. M. Peng, G. X. Cai and C. H. Zhou, *Curr. Top. Med. Chem.*, 2013, **13**, 1963–2010.
- (a) L. Zhang, K. V. Kumar, S. Rasheed, R. X. Geng and C. H. Zhou, *Chem. Biol. Drug Des.*, 2015, **86**, 648–655; (b) B. T. Yin, C. Y. Yan, X. M. Peng, S. L. Zhang, S. Rasheed, R. X. Geng and C. H. Zhou, *Eur. J. Med. Chem.*, 2014, **71**, 148–159; (c) L. Zhang, D. Addla, J. Ponmani, A. Wang, D. Xie, Y. N. Wang, S. L. Zhang, R. X. Geng, G. X. Cai, S. Li and C. H. Zhou, *Eur. J. Med. Chem.*, 2016, **111**, 160–182; (d) S. M. Clark, A. Loeffler and R. Bond, *J. Antimicrob. Chemother.*, 2015, **70**, 2048–2052.
- (a) M. Birsan, I. C. Cojocar, M. I. Stamate, V. I. Teodor and C. Tuchilus, *Rev. Chim.*, 2016, **67**, 1385–1388; (b) M. Bondaryk, W. Kurzątkowski and M. Staniszevska, *Postep. Derm. Alergol.*, 2013, **30**, 293–301; (c) B. M. Aljaeid and K. M. Hosny, *Int. J. Nanomed.*, 2016, **11**, 441–447.
- V. K. Marrapu, M. Mittal, R. Shivahare, S. Gupta and K. Bhandari, *Eur. J. Med. Chem.*, 2011, **46**, 1694–1700.
- (a) S. F. Cui, D. Addla and C. H. Zhou, *J. Med. Chem.*, 2016, **59**, 4488–4510; (b) X. J. Fang, J. Ponmani, S. R. Avula, Q. Zhou and C. H. Zhou, *Bioorg. Med. Chem. Lett.*, 2016, **26**, 2584–2588; (c) J. Ponmani, L. Zhang, S. R. Avula and C. H. Zhou, *Eur. J. Med. Chem.*, 2016, **122**, 205–215; (d) S. C. He, J. Ponmani, S. R. Avula, X. L. Wang, H. Z. Zhang and C. H. Zhou, *Sci. Sin. Chim.*, 2016, **46**, 823–847 (in Chinese).
- (a) H. H. Gong, D. Addla, J. S. Lv and C. H. Zhou, *Curr. Top. Med. Chem.*, 2016, **16**, 3303–3364; (b) H. Wang, J. Ponmani, S. Nagarajan, J. P. Meng and C. H. Zhou, *Prog. Chem.*, 2015, **27**, 704–743 (in Chinese); (c) Y. Cheng, H. Wang, D. Addla and C. H. Zhou, *Chin. J. Org. Chem.*, 2016, **36**, 1–42 (in Chinese).
- D. Gonzalez-Calderon, M. G. Mejia-Dionicio, M. A. Morales-Reza, A. Ramirez-Villalva, M. Morales-Rodríguez, B. Jauregui-Rodríguez, E. Diaz-Torres, C. Gonzalez-Romero and A. Fuentes-Benites, *Eur. J. Med. Chem.*, 2016, **112**, 60–65.
- (a) Y. Cheng, S. R. Avula, W. W. Gao, D. Addla, V. K. R. Tangadanchu, L. Zhang, J. M. Lin and C. H. Zhou, *Eur. J. Med. Chem.*, 2016, **124**, 935–945; (b) J. S. Lv, X. M. Peng, B. Kishore and C. H. Zhou, *Bioorg. Med. Chem. Lett.*, 2014, **24**, 308–313; (c) S. Li, J. X. Chen, Q. X. Xiang, L. Q. Zhang, C. H. Zhou, J. Q. Xie, L. Yu and F. Z. Li, *Eur. J. Med. Chem.*, 2014, **84**, 677–686; (d) X. M. Peng, L. P. Peng, S. Li, S. R. Avula, K. V. Kumar, S. L. Zhang, K. Y. Tam and C. H. Zhou, *Future Med. Chem.*, 2016, **8**, 1927–1940.
- (a) C. Willyard, *Nat. Med.*, 2016, **22**, 450–451; (b) C. H. Zhou and Y. Wang, *Curr. Med. Chem.*, 2012, **19**, 239–280; (c) H. Z. Zhang, G. L. V. Damu, G. X. Cai and C. H. Zhou, *Eur. J. Med. Chem.*, 2013, **64**, 329–344.
- T. Shekhar-Guturja, G. M. K. B. Gunaherath, E. M. K. Wijeratne, J. P. Lambert, A. F. Averette, S. C. Lee, T. Kim, Y. S. Bahn, F. Tripodi, R. Ammar, K. Dohl, K. Niewola-Staszowska, L. Schmitt, R. J. Loewith, F. P. Roth, D. Sanglard, D. Andes, C. Nislow, P. Coccetti, A. C. Gingras, J. Heitman, A. A. L. Gunatilaka and L. E. Cowen, *Nat. Chem. Biol.*, 2016, **12**, 867–875.
- (a) Y. Y. Zhang, J. L. Mi, C. H. Zhou and X. D. Zhou, *Eur. J. Med. Chem.*, 2011, **46**, 4391–4402; (b) J. P. Shrestha, C. Baker, Y. Kawasaki, Y. P. Subedi, N. N. Vincent de Paul, J. Y.

ARTICLE

Journal Name

- Takemoto and Cheng-Wei T. Chang, *Eur. J. Med. Chem.*, 2017, **126**, 696-704.
- 14 (a) K. Lal, C. P. Kaushik and A. Kumar, *Med. Chem. Res.*, 2015, **24**, 3258-3271; (b) S. W. Deng, C. Zhang, S. Seyedmousavi, S. Zhu, X. Tan, Y. Y. Wen, X. Huang, W. Z. Lei, Z. J. Zhou, W. J. Fang, S. S. Shen, D. Q. Deng, W. H. Pan and W. Q. Liao, *Antimicrob. Agents Chemother.*, 2015, **59**, 4312-4314.
- 15 (a) Y. Shi and C. H. Zhou, *Bioorg. Med. Chem. Lett.*, 2011, **21**, 956-960; (b) J. R. Duan, H. B. Liu, P. Jeyakkumar, L. Gopala, S. Li, R. X. Geng and C. H. Zhou, *Med. Chem. Commun.*, 2017, **8**, 907-916.
- 16 (a) X. M. Peng, G. L. V. Damu and C. H. Zhou, *Curr. Pharm. Des.*, 2013, **19**, 3884-3930; (b) X. M. Peng, K. V. Kumar, G. L. V. Damu and C. H. Zhou, *Sci. China Chem.*, 2016, **59**, 878-894; (c) G. L. V. Damu, S. F. Cui, X. M. Peng, Q. M. Wen, G. X. Cai and C. H. Zhou, *Bioorg. Med. Chem. Lett.*, 2014, **24**, 3605-3608.
- 17 (a) R. R. Zhang, J. Liu, Y. Zhang, M. Q. Hou, M. Z. Zhang, F. E. Zhou and W. H. Zhang, *Eur. J. Med. Chem.*, 2016, **116**, 76-83; (b) M. H. Shaikh, D. D. Subhedar, B. B. Shingate, F. A. K. Khan, J. N. Sangshetti, V. M. Khedkar, L. Nawale, D. Sarkar, G. R. Navale and S. S. Shinde, *Med. Chem. Res.*, 2016, **25**, 790-804; (c) D. Ashok, B. V. Lakshmi and M. Sarasija, *Lett. Org. Chem.*, 2016, **13**, 76-84.
- 18 (a) H. Z. Zhang, G. L. V. Damu, G. X. Cai and C. H. Zhou, *Curr. Org. Chem.*, 2014, **18**, 359-406; (b) G. L. V. Damu, Q. P. Wang, H. Z. Zhang, Y. Y. Zhang, J. S. Lv and C. H. Zhou, *Sci. China Chem.*, 2013, **56**, 952-969; (c) S. F. Cui, Y. Ren, S. L. Zhang, X. M. Peng, G. L. V. Damu, R. X. Geng and C. H. Zhou, *Bioorg. Med. Chem. Lett.*, 2013, **23**, 3267-3272.
- 19 S. L. Zhang, J. J. Chang, G. L. V. Damu, R. X. Geng and C. H. Zhou, *Med. Chem. Commun.*, 2013, **4**, 839-846.
- 20 National Committee for Clinical Laboratory Standards Approved standard Document. M27-A2, Reference Method for Broth Dilution Antifungal Susceptibility Testing of Yeasts, National Committee for Clinical Laboratory Standards, Wayne, PA, 2002.
- 21 (a) H. H. Gong, K. Baathula, J. S. Lv, G. X. Cai and C. H. Zhou, *Med. Chem. Commun.*, 2016, **7**, 924-931; (b) S. Q. Wen, J. Ponmani, S. R. Avula, L. Zhang and C. H. Zhou, *Bioorg. Med. Chem. Lett.*, 2016, **26**, 2768-2773; (c) D. Addla, S. Q. Wen, W. W. Gao, S. K. Maddili, L. Zhang, and C. H. Zhou, *Med. Chem. Commun.*, 2016, **7**, 1988-1994; (d) L. P. Peng, S. Nagarajan, S. Rasheed and C. H. Zhou, *Med. Chem. Commun.*, 2015, **6**, 222-229.
- 22 X. L. Li, Y. J. Hu, H. Wang, B. Q. Yu and H. L. Yue, *Biomacromolecules*, 2012, **13**, 873-880.
- 23 (a) G. W. Zhang, P. Fu, L. Wang and M. M. Hu, *J. Agric. Food Chem.*, 2011, **59**, 8944-8952; (b) H. Z. Zhang, J. Ponmani, K. V. Kumar and C. H. Zhou, *New J. Chem.*, 2015, **39**, 5776-5796; (c) L. L. Dai, H. Z. Zhang, S. Nagarajan, S. Rasheed and C. H. Zhou, *Med. Chem. Commun.*, 2015, **6**, 147-154.

Discovery of potential antifungal triazoles: Design, synthesis, biological evaluation, and preliminary antifungal mechanism exploration

Yuan Zhang,[§] Guri L V Damu,^{§#} Sheng-Feng Cui,[§] Jia-Li Mi,^b Vijai Kumar Reddy Tangadanchu[#] and Cheng-He Zhou^{*a}

^a Institute of Bioorganic & Medicinal Chemistry, Key Laboratory of Applied Chemistry of Chongqing Municipality, School of Chemistry and Chemical Engineering, Southwest University, Chongqing 400715, PR China.

^b People's Hospital of Suining, Sichuan 629000, PR China.

§ These authors contributed equally to this work.

Postdoctoral fellow from Indian Institute of Chemical Technology (IICT), India.

Synthesis of a novel triazole type of miconazole analogues as potential antifungal agents, and molecular modeling with CYP51 and experimental investigation with DNA suggested the possible antimicrobial mechanism.

